An Active Composite Pull-apart Basin Within the Central Part of the North Anatolian Fault System: the Merzifon-Suluova Basin, Turkey

BORA ROJAY & ALİ KOÇYİĞİT

Middle East Technical University, Department of Geological Engineering, Universiteler Mahallesi,
Dumplupınar Bulvarı No: 1, TR–06800 Ankara, Turkey (E-mail: brojay@metu.edu.tr)

Abstract: The North Anatolian Fault System (NAFS) that separates the Eurasian plate in the north from the Anatolian microplate in the south is an intracontinental transform plate boundary. Its course makes a northward convex arch-shaped pattern by flexure in its central part between Ladik in the east and Kargı in the west. A number of strike-slip basins of dissimilar type and age occur within the NAFS. One of the spatially large basins is the E–W-trending Merzifon-Suluova basin (MS basin), about 55 km long and 22 km wide, located on the southern inner side of the northerly-convex section of the NAFS. The MS basin has two infills separated from each other by an angular unconformity. The older and folded one is exposed along the fault-controlled margins of the basin, and dominantly consists of a Miocene fluvio-lacustrine sedimentary sequence. The younger, nearly horizontal basin infill (neotectonic infill) consists mainly of Plio–Quaternary conglomerates and sandstone-mudstone alternations of fan-apron deposits, alluvial fan deposits and recent basin floor sediments. The two basin infills have an angular unconformity between them and the deformed pattern of the older infill reveals the superimposed nature of the MS basin. The MS basin is controlled by a series of strike-slip fault zones along its margins. These are the E–W-trending Merzifon dextral fault zone along its northern margin, the E–W-trending Sarıbuğday dextral fault zone along its southern margin and the NW-trending Suluova normal fault zone along its eastern margin. The basin is cut by the E–W-trending Uzunyazı dextral fault zone, which runs parallel to the northern and southern bounding fault zones and displays a well-developed overlapping relay pattern by forming a positive flower structure. The faults of the zone cut Quaternary neotectonic infill and tectonically juxtapose the fill with older rock units. The central faults are seismically more active than the bounding faults, and are therefore relatively younger faults. The early-formed rhomboidal basin is subdivided by these E–W-trending younger faults into several coalescing sub-basins, converting it into a composite pull-apart basin. The total cumulative post-Pliocene dextral offset along the southern bounding faults is about 12.6 km.

Key Words: North Anatolian Fault System, Plio–Quaternary, composite pull-apart basin, Merzifon-Suluova

Kuzey Anadolu Fay Sistemi'nin Orta Kesimi İçinde Aktif Bir Birleşik Çek-Ayır Havza: Merzifon-Suluova Havzası, Türkiye

Özet: Kuzeyde Avrasya plakası ile güneyde Anadolu plakacığını ayıran Kuzey Anadolu Fay Sistemi (KAFS) kıta içi dönüşüm plaka sınırıdır. KAFS orta kesiminde (doğuda Ladik ile batıda Kargı arasında) kuzeye bakan bir yay oluşturur. KAFS içinde çok sayıda değişik tür ve yaşlı doğrultu atımlı havza yer alır. Alansal dağılımı büyük olan havzalardan biri Merzifon-Suluova (MS) havzasıdır. MS havzası, KAFS'nin orta kesimindeki yayın güney iç kesiminde yer alır. DB uzanımlı MS havzası yaklaşık 55 km uzunluğu ve 22 km genişliğindedir. MS havzası birbirlerinden açısal uyumsuzluk ile ayrılan iki havza dolgusu içerir. Daha yaşlı ve kıvrımlanmış olan havza dolgusu havzanın faylarla denetlenen kenar kesimlerinde yaygın olarak yüzeyler ve egemen olarak Miyosen yaşlı göl-akarsu ortamında çökelmiş sedimanter bir istiften oluşur. Genç Pliyo–Kuvaterner, hemen hemen yatay konumlu olan çakıltaşı ve kumtaşı-çamurtaşı ardaşımından oluşan dolgu (yenitektonik dolgu) ise yelpaze-önlük tortulları, yelpaze tortulları ve güncel havza tabanı sedimanlarından oluşur. Bu iki havza dolgusu, dolgular arasındaki açısal uyumsuzluk ve daha yaşlı dolgunun deformasyon biçimi, MS havzasının üzerlemiş niteliğini gösterir. MS havzası, kenarları boyunca bir seri doğrultu atımlı fay kuşağı tarafından denetlenir. Bunlar havzanın kuzey kenarını sınırlayıp denetleyen D–B gidişli Merzifon doğrultu atımlı fay kuşağı, havzanın güney kenarını belirleyip denetleyen Sarıbuğday sağ yanal doğrultu atımlı fay kuşağları, ve havzanın doğu kenarını sınırlayıp denetleyen KB gidişli Suluova normal fay kuşağıdır. Bunların dışında, havzayı kesen ve evriminde önemli rol oynayan iki fay daha vardır. Bunlar D–B gidişli Uzunyazı sağ yanal doğrultu atımlı fay kuşağıdır. Havzayı sınırlıyan faylara parallel gelişen ve pozitif çiçek yapısı sunan bu fay kuşağı Kuvaterner yaşlı yenitektonik dolgusunu

öteler ve onu daha yaşlı birimlerle tektonik olarak karşı-karşıya getirir. Bu faylar, aynı zamanda sismik olarak da etkin olup, diğer kenar fay kuşaklarından çok daha gençtir. Daha önce oluşmuş, eşkenar dikdörtgen biçimli bu havza, bu genç faylar tarafından birkaç birleşik alt havzaya bölünerek, birleşik havza türünde yeni bir havzaya değişimine yol açmıştır. MS üzerlemiş-birleşik çek ayır havzasının gelişimi sırasında, havzanın güney kenar fayları boyunca birikmiş olan toplam sağ yanal doğrultu-atım miktarı Pliyosenden bu yana yaklaşık 12.6 km olarak bulunmuştur.

Anahtar Sözcükler: Kuzey Anadolu Fay Sistemi, Pliyo–Kuvaterner, birleşik çek-ayır havza, Merzifon-Suluova

Introduction

The recent configuration of Anatolia and its surrounding region is configured by the westward continental escape of the Anatolian microplate, resulting from the post-collisional convergence of the African-Arabian and Eurasian plates. The convergence resulted in the migration of the Anatolian microplate on to the African plate along the Eastern Mediterranean 'ridge' (Şengör 1980; Allen 1982). That neotectonic framework of Anatolia is characterized by great variety of deformational structures, the largest of which are two strike-slip fault systems. These two major intracontinental transform faults shaping Anatolia are the dextral North Anatolian and sinistral East Anatolian fault systems (Figure 1). The development of a series of western Anatolian grabens and intraplate deformations are the results of the escape of the Anatolian Plate between these two

intracontinental transform faults (Şengör & Yılmaz 1981).

Several relatively narrow elongated depressions are aligned parallel or subparallel to these transform fault zones. However, the basins situated in the intraplate domains between the major splays and the master strand of the North Anatolian Fault System are much more complex and problematic; for example the Merzifon-Suluova basin (MS basin) (Figure 2) or the Çerkeş-Kurşunlu and Tosya basins (Barka & Hancock 1984; Barka 1992), unlike those lying along the fault zones. Such basins are much larger than those along the seismogenic master fault zone.

The MS basin that is the subject of this paper is located north of the Ezinepazarı-Sungurlu splay fault (Blumenthal 1950; Aktimur *et al.* 1990; Bozkurt & Koçyiğit 1996) and south of the seismically active North Anatolian Fault Master Strand (NAFMS)
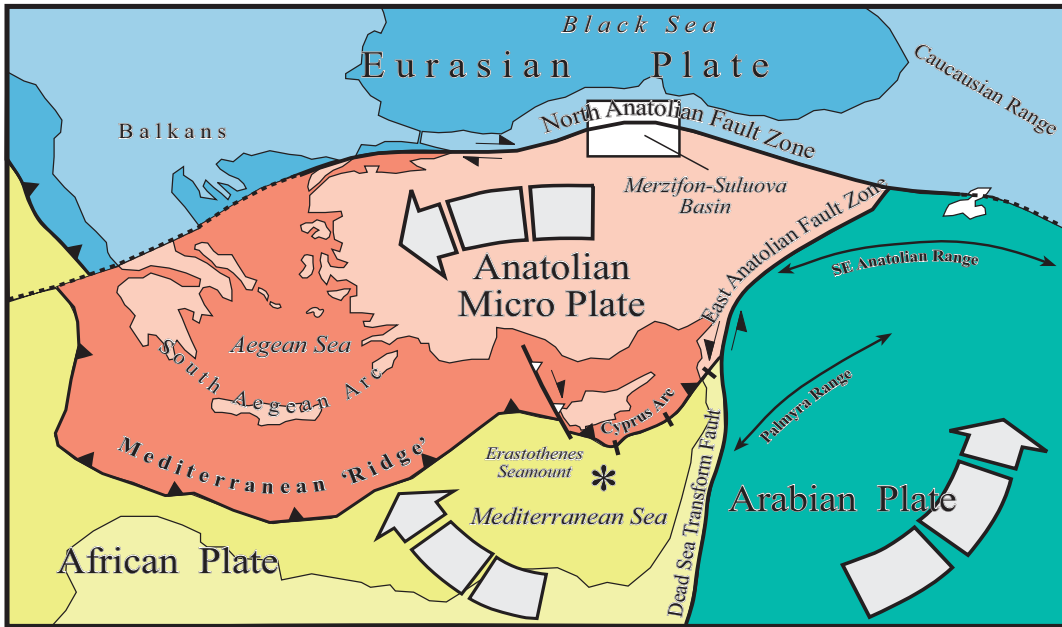

Figure 1. Neotectonic setting of the Eastern Mediterranean and the Merzifon-Suluova Basin.
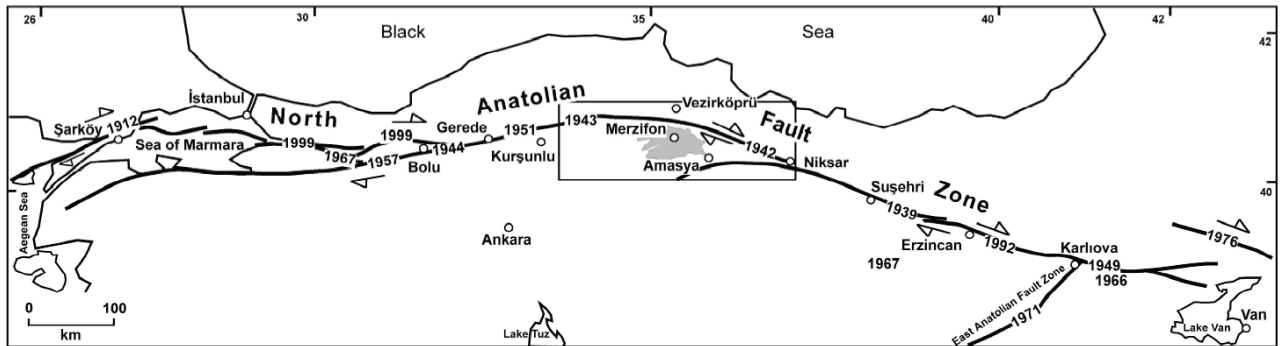
Figure 2. Seismic events along the Master Strand of the North Anatolian Fault Zone and the position of the MS Basin.

(Blumenthal 1945, 1950; Dirik 1994; Şengör *et al.* 2005). The rhomboidal basin, 55 km long and 20–22 km wide, with its long axis trending E–W (Figures 2 & 3) has been interpreted as a basin developed in a strike-slip regime as a complex pull-apart basin or composite pull-apart basin (Koçyiğit & Rojay 1988; Rojay 1993; Rojay & Koçyiğit 2003).

The seismic activity of the region was manifested by recent earthquakes (1985, 1992, 1996, 1997 Amasya-Çorum earthquakes; Demirtaş 1996; http://www.koeri.boun.edu.tr). This seismic activity along the faults is supported by aerial photographic surveys (Arpat & Şaroğlu 1975) and geophysical surveys done in the MS basin (DSİ Report 1973).

The purpose of the article is to discuss the neotectonic evolution of this seismically active MS basin during Plio–Quaternary time.

Stratigraphy

The tectonostratigraphic units of the region, distinguishable by their age, lithostratigraphic evolution, internal organization and tectonic position, are grouped into various rock sequence packages (Blumenthal 1950; Alp 1972; Seymen 1975; Öztürk 1980; Rojay 1995; Tüysüz 1996). The basic differentiation is based on the attitude of the sequences, or whether they are allochthonous or autochthonous. The pre-Campanian units comprise pre-Liassic low-grade metamorphic rocks, a Triassic sedimentary complex, Jurassic–Cretaceous clastics and carbonates, and Cretaceous ophiolitic mélange which are all allochthonous. The unconformably overlying Campanian–Quaternary units, relatively autochthonous, mainly comprise a Campanian–Maastrichtian fore-arc flysch sequence with extensive volcanics and mafic dykes, Eocene molassic sediments filling the rift, to peripheral basinal sequences with volcanics and dacitic intrusions, Miocene lacustrine mudrocks and Pliocene–Quaternary fluvial deposits (Figure 4).

Within this stratigraphic frame, the Pliocene–Quaternary fluvial deposits studied in this paper are the neotectonic fill of the MS basin. These fluvial deposits are probably the coeval units of the 'Pontus' Formation (Irrlitz 1971; Barka 1984) distributed throughout the Central Pontides. The neotectonic basin fill of the MS basin predominantly consists of fluvial to lacustrine clastics of Pliocene–Quaternary age (Sickenberg & Tobein 1971; Sickenberg *et al.* 1975; Genç *et al.* 1993; Rojay 1993). It overlies unconformably all the pre-Pliocene units (Figure 5) and is over 410 m thick (subsurface data of the Hydraulic and Water Resource Department [DSİ Report 1973] and Mineral Research and Exploration Institute reports [Genç *et al.* 1993]).

The neotectonic fill displays different lithologies with different relations with the underlying older units. Generally coarser alluvial fan deposits overlying Miocene green mudrocks characterize the neotectonic basin fill of the MS basin (Figures 4 & 5). Its stratigraphic relations suggest a Plio–Quaternary age. The red units are generally fluvial to alluvial fan deposits, affected by syn-sedimentary small-scale normal faults and post-Miocene faulting. The thicknesses of the alluvial fans may be up to 350 m thick in some places controlled by these faults near Merzifon (DSİ Report 1973). The fill on
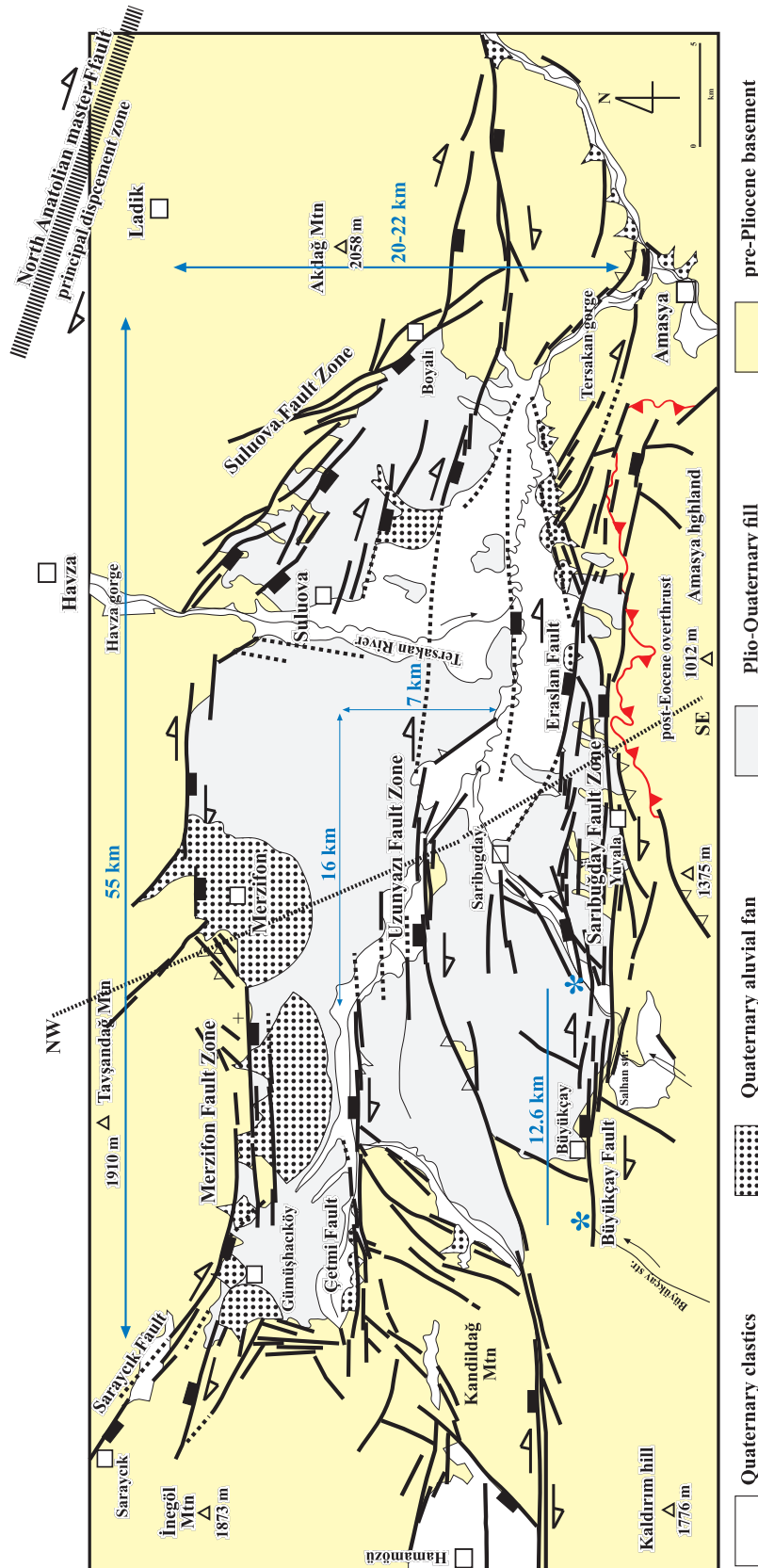
Figure 3. Neotectonic map of the MS Basin showing the size of basins and the location of NW–SE cross-section (see Figure 7).

AGE	UNIT	Thickness (m)	LITHOLOGY	DESCRIPTION	DEPOSITIONAL SETTING
Q		>2		fluvial terrace conglomerates, travertines, alluvial fans, alluvium, swamp, ...	alluvial fan to fluvial
				unconformity	
PLIOCENE-QUATERNARY	SULUOVA GROUP	25		alternation of yellow-yellowish brown, medium-thick-bedded sandstones and conglomerates with greyish white massive conglomerates — reddish, medium-bedded sandstones and massive conglomerates	lake shoreline
		21		fining-upward sequence; alternating yellowish brown, medium- to thick-bedded siltstones, sandstones and conglomerates with greyish white and red massive conglomerates — minor gypsum beds with coal laminations	swamp-lake
		42		red, reddish brown massive polygenetic conglomerates with red, medium-bedded sandstones and reddish brown marls — yellow sandstones with thick-bedded polygenetic conglomerates	fluvial
		57		alternation of red-reddish brown, medium- and cross-bedded sandstone-siltstone sequence and red-purple, medium-beddded to massive polygenetic conglomerates with red conglomerate lobes — red channel conglomerates — red to purple massive polygenetic conglomerates with red medium-thick-bedded sandstone-siltstone sequence	alluvial fan to fluvial
				unconformity	
Pre-PLIOCENE	Miocene Units / Eocene Units	>17		**Miocene mudrocks** — alternation of light green clastics; dominantly thin-medium-bedded mudrocks with minor cross-bedded sandstones, horizons of mammal bones, teeth and plant remains, gastropoda and coal beds	accreted basins and accretionary complex — Miocene Lake
				unconformity	
				pre-Neogene basement — Cretaceous-Palaeogene accretionary complex — Middle-Upper Eocene sequence	Middle-Upper Eocene sequence

Figure 4. Tectonostratigraphy of the MS Basin.

the eastern margin of the MS basin starts with red conglomerates and sandstones measuring up to 64 m thick, unconformably overlying Lutetian clastics and Miocene mudrocks. Based on their stratigraphic position, the age of the red units is accepted as Plio–Quaternary. The sandstones and conglomerates gradationally overlying the red clastics have a limited distribution at the eastern margin of the MS basin with a maximum measurable thickness of over 83 m. The sequence displays a continental depositional
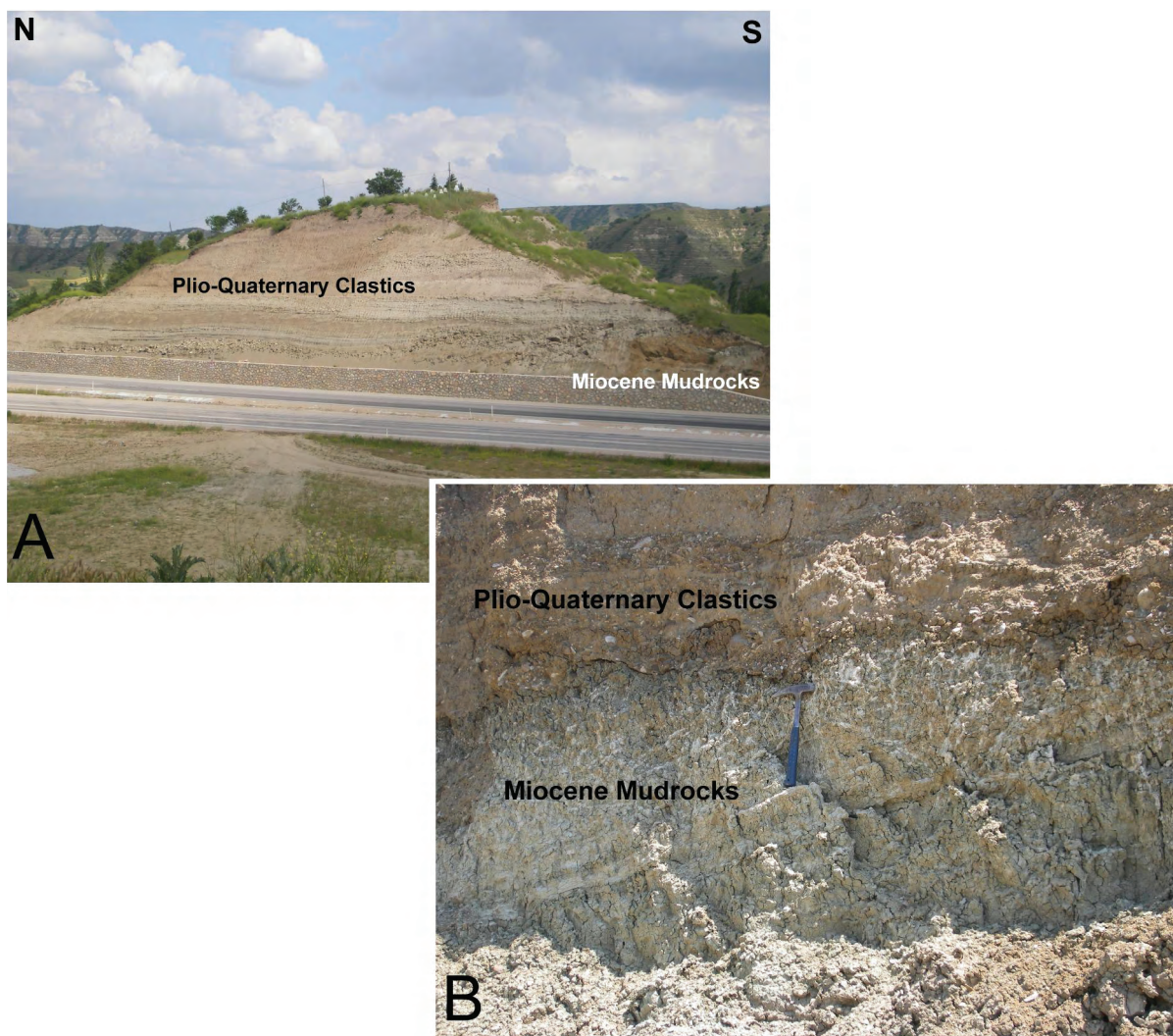
Figure 5. The unconformity between highly deformed Miocene mudrocks below and almost horizontal Plio–Quaternary clastics above. Location: A– Kamışlı-Merzifon road cut, B– Suluova section.

setting of both lacustrine and fluvial environmental inputs. Borehole data suggests that the total thickness of the eastern margin Plio–Quaternary clastics exceeds 147 m. The central basinal sequence consists predominantly of green mudrocks and cross-bedded sandstones-siltstones with a measurable thickness of over 59 m. The stratigraphic relations and palaeontological data support a Pliocene–Pleistocene age (Genç *et al.* 1993; Rojay 1993). The basinal mudrock sequence manifests a moderately anaerobic, lacustrine depositional setting with minor fluvial current influx.

The southern margin of the basin consists predominantly of pale clastic rocks. It unconformably overlies all the pre-Pliocene units and is unconformably overlain by uppermost Quaternary sediments. The maximum measured thickness of the formation is over 39 metres at the southern margin. The unit has an almost uniform distribution and stratigraphic evolution along the southern margin. However, to the southwest, coarser clastics dominate the Plio–Quaternary sequence (Villafranchium) (Sickenberg & Tobein 1971; Sickenberg *et al.* 1975; Genç *et al.* 1993). The depositional environment

of the sequences has been interpreted as a fluvial-terrace to lacustrine setting. The unit was deposited along the southern margin of a lake and periodically affected by the activity of basement involving normal faulting (Rojay 1993).

As a whole, the Pliocene–Quaternary basin fill reveals a fluvial to lacustrine depositional setting with no volcanic influx.

The Uppermost Quaternary units consist of talus breccias and seasonal fluvial sediments, alluvial fan sediments, travertines, braided and meandering river-plain deposits, terrace conglomerates and swamp deposits which all are presumed to be coeval deposits. The thicknesses of the uppermost Quaternary basin fill change from a few metres up to over 10 metres. However, the thickness of the Quaternary alluvial fans in Merzifon (northern margin) reaches up to hundreds of metres (DSİ Report 1973).

Tectonics

Tectonic evolution is discussed where palaeotectonic and neotectonic headings are differentiated from each other by angular unconformity at the base of the Pliocene units (Figure 5) and there is a deformational intensity difference between the uppermost Miocene and Pliocene units of the MS basin.

Palaeotectonic Structures

The most striking palaeotectonic structures are the duplex overthrusts caused by the emplacement of the mélanges during Mesozoic–Paleogene orogenies. The overthrust belt that is worth mentioning here extends in a curvilinear pattern from Gerne village in the west in N68°E to almost E–W and bends to about N36°W at Amasya in the east for more than 32 km in a zone of 10 km. Along the overthrust belt, the Palaeozoic metamorphics, Jurassic–Cretaceous carbonates and Cretaceous ophiolitic units within accreted mélanges were all thrust on to Lutetian sequences and transported northward at least 5 km along a low-angle overthrust plane dipping south with top-to-the-north vergence (Rojay 1993, 1995).

The youngest record of palaeotectonic activity is the thrusting of the Jurassic–Cretaceous carbonates onto Miocene mudrocks east of Çaybaşı village (Figure 6).

Neotectonic Structures

The structures developed in the Plio–Quaternary and the Quaternary units are presumed to be neotectonic structures caused by the compressional-extensional (transtensional) regime operating since the latest Miocene–Pliocene in northern Anatolia (Ketin 1969; Tokay 1973; Şengör et al. 1985, 2005; Koçyiğit 1989; Barka 1992). The neotectonic structures observed in the basin are grouped and analyzed as folds and faults.

Folds

The average strike of the fold axes in Pliocene–Quaternary sequences is N85°E to E–W, statistically calculated from the bedding attitudes of the Plio-Quaternary units (Rojay 1993). Based on the trend of fold axes, three groups of folds were distinguished. The first group of folds was observed in the centre and at the southern margin of the basin and strike N80–85°E and N80°E, respectively. They are parallel to the strikes of the marginal faults (Figure 5). The second group of folds, observed at the eastern margin of the basin, have axial trends of N65–70°W (Figure 5). They are also parallel to the strike of eastern margin faults. However, a relatively older, third group of folds trending N10–20°E and oblique to the strike of major faults were observed at the southern and eastern margins of the MS basin. These folds are interpreted as bends developed under the effect of buried basement faults. Upper Quaternary sediments of the basin are mostly fault bounded and tilted by up to 10° at several locations. No folding was observed within these units.

Faults

The neotectonic faults bordering and dissecting the basin will be discussed as groups of faults; (i) Merzifon Fault Zone and Çetmi Fault (northern margin faults), (ii) Suluova Fault Zone (eastern margin faults), (iii) Uzunyazı Fault Zone (central fault zone), and (iv) Sarıbuğday Fault Zone (southern margin faults) (Figures 3 & 7).

Merzifon Fault Zone and Çetmi Fault – The northern margin faults consist of separate subparallel
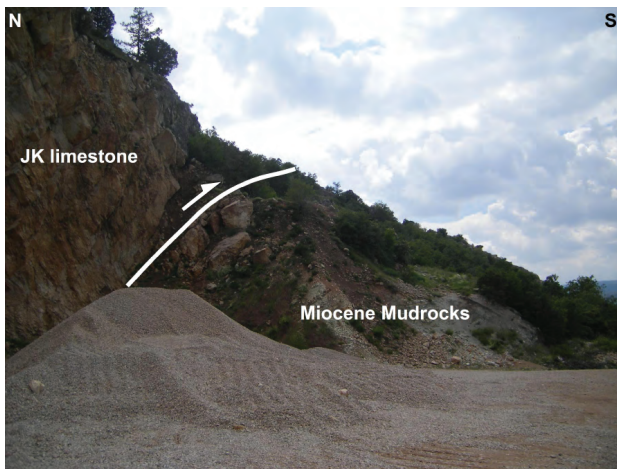
Figure 6. The youngest compressional structure, a thrust, where Jurassic–Cretaceous carbonates are thrust southwards on to Miocene mudrocks. Location: SE of Çaybaşı village.

fault sets trending almost E–W. One of these faults bounds the MS basin on the north (Merzifon Fault Zone) and the other one lies north of the central uplift (Çetmi Fault) forming a trough between them (Figures 3 & 7).

The Merzifon Fault Zone extends for over 51 km trending N40°W and E–W in a zone of a few m to 5 km wide. The fault zone splayed from the NAFZ trending N 40–45° W for over 10 km as series of strike-slip faults and continues trending N60°W to N75°W, controlling the evolution of a Late Quaternary basin around Saraycık village (Figure 3). Within the MS basin the faults trend N80°W to E–W and control the

northern margin of the MS basin. Morphologically steep slope, thick alluvial fans, dextrally diverted streams/creeks, triangular facets, young linear troughs, topographic trenches, and strike-slip fault plane slip data are the most striking manifestations of the faults, besides the uplift of the northern blocks of the fault (footwall) where the basement rocks are exposed (Tavşandağı push-ups). Some of the faults are documented by geophysical surveys (DSİ Report 1973) and it was also documented there that the northern blocks are elevated. The faults allowed the deposition of over 410 m of Plio–Quaternary clastics (DSİ Report 1973). To the east, the faults continue northwards by bending to N60°W, N85°W and N72°W for about 12 km in a zone of maximum 2 km width. The Merzifon Fault Zone joins the N45°W-trending Suluova fault zone at its eastern end.

The Çetmi Fault, south of the Merzifon Fault Zone, trends E–W for over 20 km in a fragmented pattern and fans out trending N80°E and N56°E for 4 km (Figure 3). The pre-Plio–Quaternary basement rocks are exposed along the faults, especially in the western segment of the southern faults, where the southern blocks are elevated (Kandildağ horst). The fault scarp manifestations are not very clear, although triangular facets, dextrally diverted topographic ridges, a series of small, thick and steep-slope alluvial fans and dextrally diverted creeks/streams are indications of Quaternary displacement. Along these faults, Plio–Quaternary rocks are raised up to 52 m. The uplift amount decreases from west to
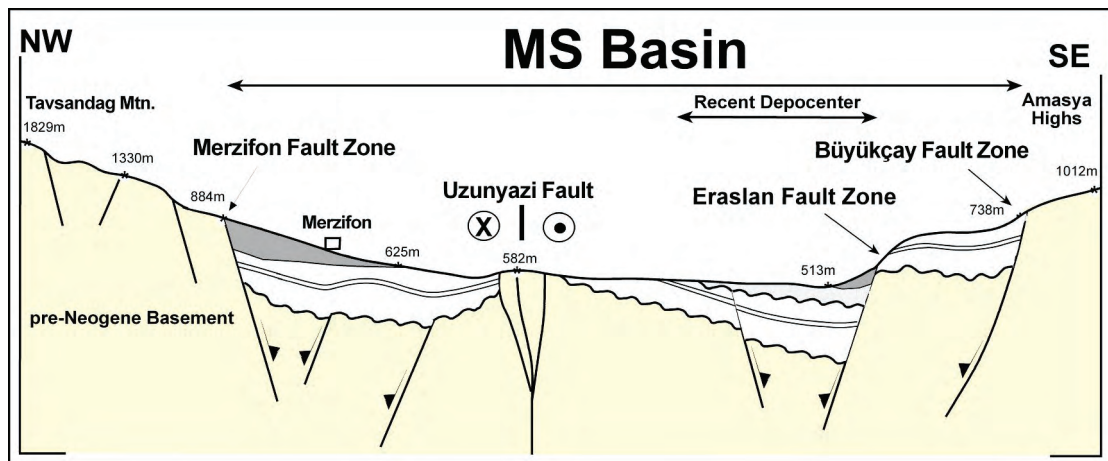

Figure 7. Geological cross-section showing the neotectonic faults and basinal components. See Figure 3 for location.

east, suggesting a scissor-like faulting with dip-slip normal components. The faults structurally control the development of the trough-like Quaternary valley of the Gümüşsuyu stream. The thickness of the Plio–Quaternary fill is 110–138 m (DSİ Report 1973), indicating a structural control of the basin fill deposition. The faults were well defined by geophysical surveys where the northern blocks are downthrown (DSİ Report 1973).

The NW margin of the MS basin is controlled by series of parallel, N15°E to N–S-trending oblique-slip normal faults in a zone 3 km wide and 5 km long southwest of Gümüşhacıköy (Figure 3). The fault set gave rise to the development of an extensional area between the Merzifon Fault Zone and the Çetmi Fault. The thickness of the Plio–Quaternary sequence is 50–60 m at the margins and 80–90 m to 138 m towards the basin centre between the Merzifon Fault Zone and the Çetmi Fault (DSİ Report 1973).

Suluova Fault Zone – A sudden break in topography and the Plio–Quaternary–Recent fill distribution differentiate the eastern margin faults (Figure 3). The fault zone extends over 27 km from northwest of Suluova village to the eastern end of the Uzunyazı fault zone, is up to 7 km wide and trends N62°W to N30°W (Figure 3). Within this zone, the eastern belt controls the Plio–Quaternary configuration and the southwestern belt of N60°W to E–W-trending faults, controls the Quaternary configuration. The major faults within this zone are linked to each other by N15–25°W-trending small-scale en-échelon faults (Figure 3). The pattern of the N62°W to N30°W-trending master faults displays a step-like pattern. The northeastern blocks are elevated, with the basement rocks exposed along faults (e.g., NE of Suluova town). The Quaternary terrace conglomerates are elevated to maximum heights of 40 m and tilted up to 20°. The fault scarps are well developed with normal dip-slip fault plane markings (normal faults with strike-slip components). The active landslides and earthquake epicentre distributions are indications of seismic creep along this zone. Some villages are damaged after each earthquake affected the region along these faults (e.g., Boyalı village).

Uzunyazı Fault Zone – This 1-km-wide fault zone extends for more than 150 km from far west of Laçin in the west, through the centre of the MS basin to Taşova in the east where it joins the NAFZ (Figures 2 & 3). The fault zone is defined in three segments within the basin (Figure 3).

The western segment faults extend from Laçin trending N85°W to E–W to N65°E for 34 km within the study area where the southern blocks are raised. In the southern blocks, pre-Plio–Quaternary basement rocks are exposed. However, in the central parts of this fault segment, the faults cut the basement rocks where no Plio–Quaternary sediments are present. The fanning of faults towards the eastern tip of the fault zone resulted in the formation of push-ups, with pre-Plio–Quaternary basement rocks exposed. The surface manifestations are northward-dipping high angle fault scarps (85–90° N). The Plio–Quaternary units are exposed where the surface manifestations indicate a dextral displacement along these faults.

The central segment of the Central fault zone, previously recognized by the DSİ team (DSİ Report 1973) (Figure 3), was later interpreted as an active fracture based on aerial photo studies (Arpat & Şaroğlu 1975). The E–W-trending set bends southeast. This bifurcating fault set consists of many short fault segments and linear troughs. The southern block, more than 22 km long, is elevated along the main central segment. In the southeasterly continuation of the fault segment, the northern blocks are elevated where they bound the actual depocentre on the north (Figure 3). Dominant diagnostic features related to each fault are the dextrally diverted curvilinear topographic ridges which are oblique or almost perpendicular to the faults, throws of up to 0.5–2.0 m in Quaternary deposits, elevated terrace conglomerates which lie 20 to 40 m above the recent alluvial plain deposits and 'tilted' terrace conglomerates. The fault is a dextral strike-slip fault with high-angle normal components that forms a positive flower structure (Harding & Lowell 1979) (Figures 7 & 8).

The faults of this segment are linked by overstepping faults trending N32°W, with terrace conglomerates elevated by about 30–40 m. Uplifted and 'tilted' Quaternary terrace conglomerates and a sudden break in the slope angles suggest that the faults are still active.
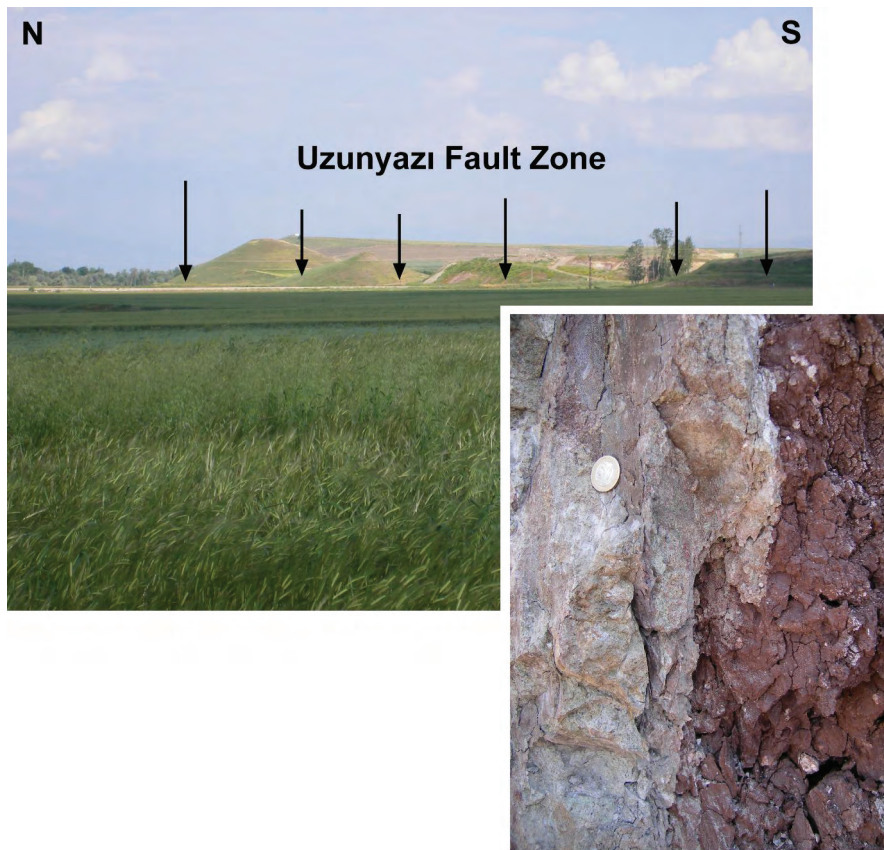
Figure 8. General view of the Uzunyazı Fault Zone and shared zone. Location: E of Uzunyazı village.

The eastern segment faults extend for more than 19 km from S of Suluova to Taşova in the far east of the study area (Figure 3). This segment consists of several stepovers, subparallel- to parallel-trending vertical faults resulting in a 700 m wide subzone. Diagnostic features are tilting of the Plio–Quaternary deposits from 21° up to 80° and terrace conglomerates up to 11°, shifted topographic ridges, triangular facets and uplifted terrace conglomerates (up to 40 m).

On this curvilinear pattern of the fault zone, the western sector of the Uzunyazı fault is a restraining bend where the southern block is thrust on to the northern one and the eastern part is a releasing bend where northern blocks are uplifted and a narrow linear depression is developed (Figure 3). As a whole, this active fault set displays dextral strike-slip faulting; (i) high-angle reverse components trending N65°E in the western segment where the southern blocks are elevated, (ii) high-angle normal components in E–W-trending faults in the central segment where the southern blocks are elevated, and (iii) normal components in N64°W-trending faults in the eastern segment where the northern blocks are uplifted (Figure 3).

The central fault zone displays a positive flower structure, a strike-slip fault with dextrally displaced topographic ridges and dextral fault plane solutions.

Sarıbuğday Fault Zone – The sudden break in topography and Quaternary–Recent fill distribution force us to differentiate the southern margin faults into two major parallel fault belts. The fault zone extends for over 54 km, trending E–W to N76°W, from west of Büyükçay village to Amasya in a zone up to 6 km wide. Within this zone, the northern belt controls the Quaternary configuration (Eraslan Fault subzone) and the southern belt controls the Plio–

Quaternary configuration (Büyükçay Fault subzone) of the MS basin (Figures 3 & 7).

Eraslan Fault Subzone – The Eraslan faults borders for 25 km the southern margin of the Quaternary part of the MS basin where the southern block is uplifted. The fault set consists of 3 main segments. The western segment consists of several faults, trending N70°W and N86°W, affecting Plio–Quaternary and Quaternary units. The main fault segment that trends N80°W consists of right-overstepped faults. Along the further east continuation of the fault segment, dextral strike-slip manifestations were recorded on N82°W striking, 80°N dipping fault planes. In particular, the central segment displays a tectonically young morphology with triangular facets, uplifted terraces and dextrally offset creeks. The fault zone bends and continues with N60–75°W-trending faults in the east. This part consists mainly of faults with elevated southern blocks, displaying well-developed north-facing step like morphologies (Figure 9) which fully control the actual depocentre from the south. The alignment of alluvial fan distribution is one of the main characteristics of this segment. The other diagnostic fault-related features are mechanical surfaces (brecciation, recrystallization and Fe-oxidization) on the JK carbonates and 10 to 28 m uplifted travertine occurrences whose natural formation has already been stopped. This fault subzone generally displays dextral strike-slip faulting with a normal-slip component.

Büyükçay Fault Subzone – The southern belt controls the Plio–Quaternary configuration from Büyükçay village in the west for 54 km to Amasya in the east (Figure 3). The E–W-trending southwestern faults extend for 23 km where the southern blocks are uplifted (Figures 3 & 10). The faults structurally control the Salhan and Büyükçay streams. Along this fault, the courses of streams were dextrally displaced by up to 875 m since the latest Quaternary. Total dextral displacement of the Salhan stream was measured at 12.6 km (Figure 11) where the 1996 earthquake (Salhançayı earthquake 1996; Demirtaş 1996) possibly took place along this fault (Figure 3). To the east, the faults continue eastwards to Yuvala

Figure 9. Paired terrace conglomerates showing two phases of downthrow along the southern margin. The equivalent fluvial terraces are dated between 109±7.4 ka and 32.4±4.4 ka (Kıyak & Erturaç 2008). Location: SW of Eraslan village.
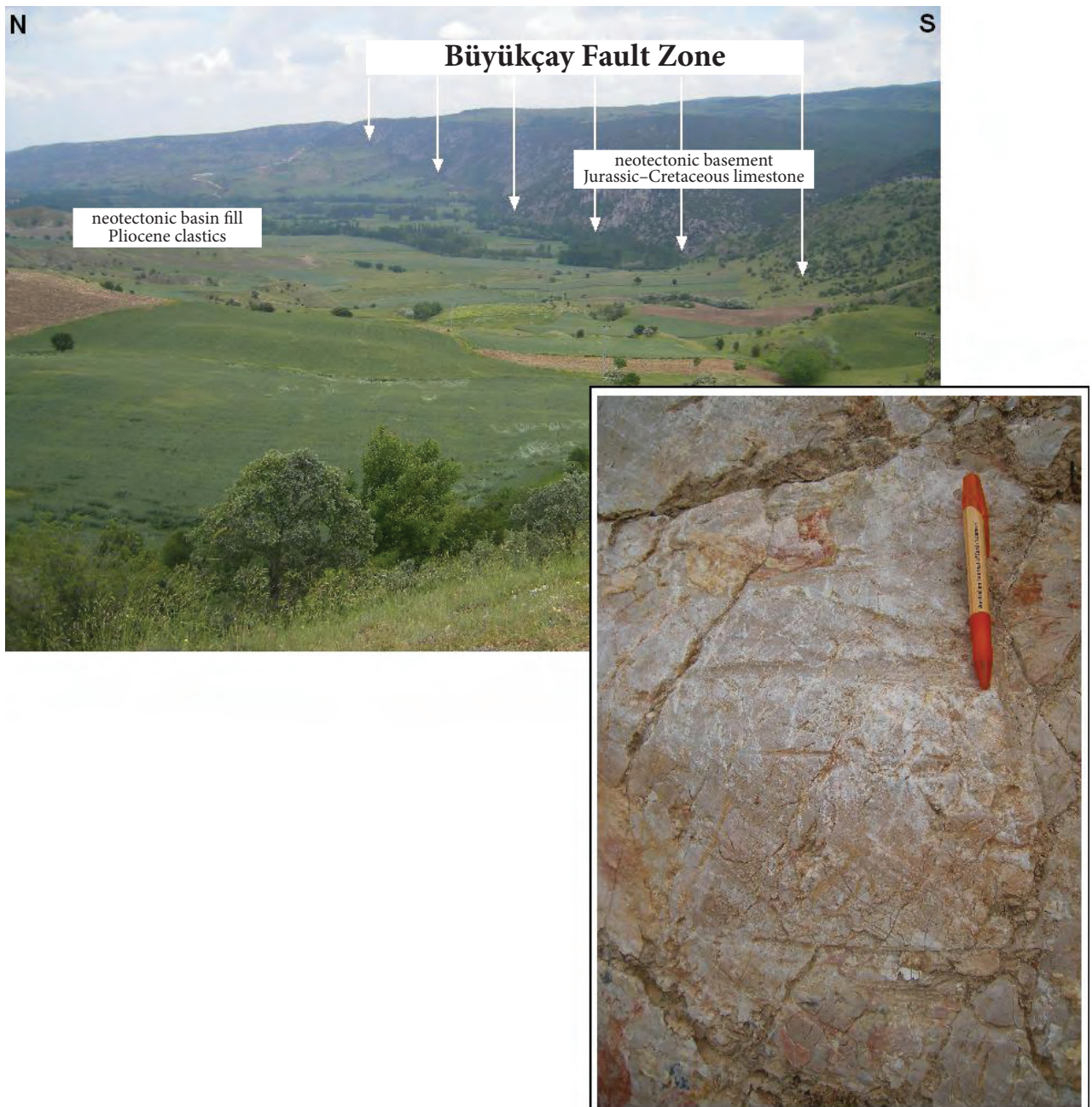
Figure 10. General view of the Büyükçay Fault Zone and dextral strike-slip data overprinted onto normal and reverse faulting. Location: SE of Çaybaşı village.

village and bifurcate in N50–76°E directions. The bifurcating faults consist of almost E–W-trending overstepping faults and N50–76°E-trending fanning-faults. Along these N85°E to E–W-trending faults where the southern blocks were uplifted, the course of the stream was dextrally displaced by around 475–550 m since the Latest Quaternary. Out of five

faults crossing the Bulanık stream, the ratios of fault lengths to the offset along streams calculated along the southwestern margin faults are 0.083 to 0.088. The offset is right-lateral. This result indicates that each fault was activated at the same time. The central faults of the fault zone consist of several stepovers and parallel faults, and extend for 20 km. There are three
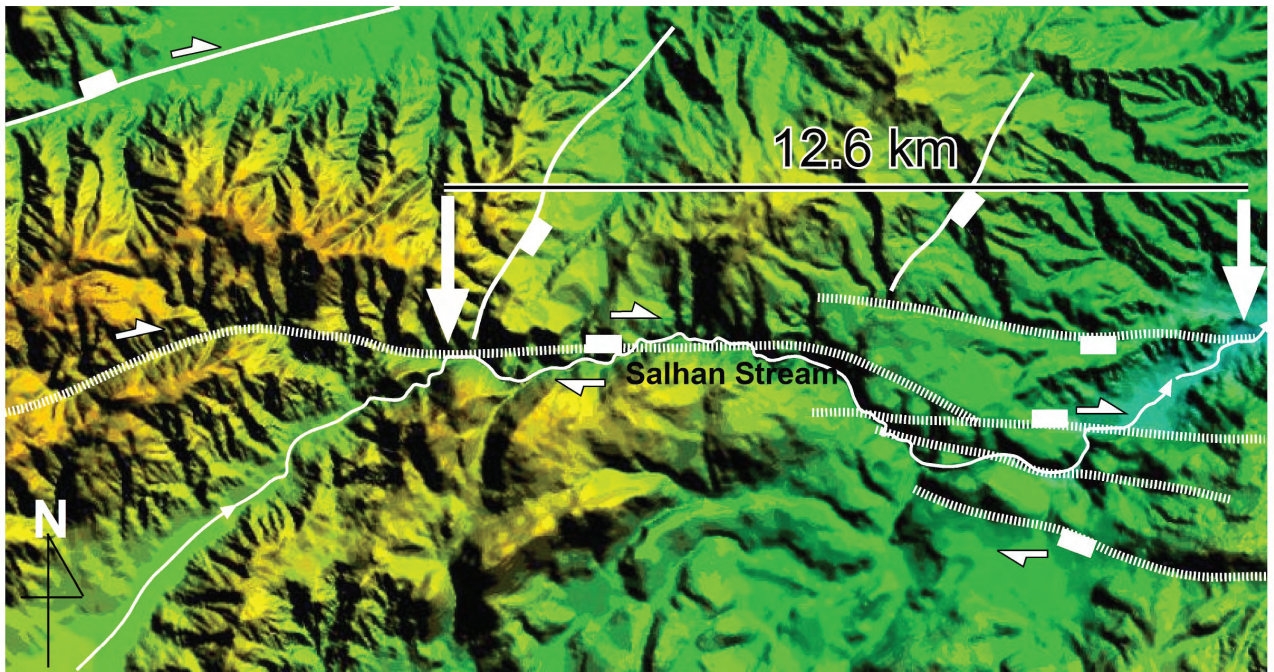
Figure 11. DEM showing displacement of 12.6 km since the Pliocene along the Büyükçay Fault Zone.

main sets of faults; E–W-trending, N80°E- to E–W-trending and N80°W-trending faults. The E–W-trending faults form a horst between N75°W and N86°E trending faults west of Yuvala village where the Plio–Quaternary units were tilted up to 24°. Elevation differences of up to 50 m in the attitudes of the Plio–Quaternary units are indications of the latest movements along these faults. The southern block of the N80°E- to E–W-trending central fault was elevated and bounds the southern margin of the MS basin for 7 km. Along this fault, Plio–Quaternary units are preserved on uplifted southern blocks with a fresh fault scarp, forming north-facing triangular facets to the west of Yuvala. Along the fault line, the Plio–Quaternary units were tilted up to 24°. There is no direct evidence for its lateral movement besides its vertical movement. The N80°W-trending fault extends for 8 km where the northern block was uplifted. The eastern termination of the fault is concealed under Quaternary talus and terrace conglomerates. The southeastern faults consist of several minor short, subparallel, parallel and stepover faults trending N60°W to N75°W for 16 km in a zone 4 km wide. The southern blocks of the faults were mainly elevated and dissected by N–S- to N10°W-trending right-lateral oblique-slip faults. The Plio–Quaternary units were tilted up to 10° at the edges of the uplifted southern blocks. Within this belt, a travertine, already completely formed, was observed at the junction of northwest-trending and N–S-trending right-lateral strike-slip faults. The youngest movement recorded is dextral strike-slip faulting which overprints earlier reverse and normal faulting.

Neotectonic Characteristics of the Merzifon-Suluova Basin

Morphotectonics

The MS basin is a 55-km-long and 20–22-km-wide rhomboidal depression with its long axis parallel to the NAFMS (Figures 2 & 3). The basin is divided into several small combined pull-apart depressions of Quaternary age (Figure 3).

Relative vertical uplifts and lateral movements between the faulted blocks have increased the topographic gradients and elevation differences along the margins (Figure 7). At the northern margin of the basin, the highest topographic peak (N of Merzifon town) reaches 1900 m and the lowest elevation at

the northern margin of the basin is 884 m, so the resulting topographic elevation difference is 1016 m. In the same way, the topographic elevation difference at the western margin is 1123 m; at the SW margin, 559 m; at the southern margin, 447 m and 671 m, and at the eastern margin it is 559 m. The maximum vertical uplift along the central fault zone is measured at 72 m.

The slopes of the margins are 10° on the basement rocks and 2° on the neotectonic fill at the northern margin, 13° and 1.2° at the western margin, 7° and 1.7° at the southern margin and 9° and 3° at the eastern margin. As is clear from this, the uplift of the northern margin (Tavşandağ push-up) is relatively much higher than the southern margin (Amasya Highs) (Figure 3). Therefore the alluvial fans resting on the northern margin are much thicker and more extensive than the alluvial fans on the other margins of the basin. The actual alluvial fans deposited on northern and southern margins of the MS basin indicate active uplift on the southern and northern margins. The rate of uplift along the northern margin faults (Merzifon faults) must be much faster than on the southern margin faults (Eraslan faults) (Figure 7).

The gentle slopes are the result of long-term retreat of fault scarps and triangular facets, and well-developed alluvial fan/apron/plain interactions. These may indicate a relatively slow tectonic movement or rapid erosion and sedimentation relative to fault activity, or both.

Displacements

Vertical uplifts and strike-slip motions are the major displacements recorded in the MS basin. Of the several streams flowing from the mountains to the basin, most die out and leave their load on alluvial fans or along the fault lines. As they enter the basin, they are structurally controlled by the faults. The largest one, the Tersakan stream, flows southwards across the basin as a braided stream for 15 km, then turns sharply and flows N75°W as a meandering stream when it enters the actual depocentre along the fault line (Figure 3). The stream has a sinistral sense of shift which results from the tilt of the actual depocentre.

However, almost all the streams along the southern margin are displaced dextrally. The

stream flowing northwards to Sarıbuğday village is displaced dextrally many times. The cumulative dextral displacement along the southern margin faults is about 12.6 km with 160 m vertical uplift (since the Pliocene) and 500–550 m with 10–28 m vertical uplift (since the latest Quaternary). The faults, having almost the same trend, displaced the stream by different amounts depending on the fault lengths. However, there is a constant ratio between the length of the faults and the displacement amounts of the stream courses. The ratio of length of fault to displacement along streams was found to be 0.085 (0.0813–0.0875), which indicates that the faults are evolving at the same time. Knowing this relationship, it can be concluded that all the faults developed along this belt evolved during the same period. Along this belt, the Salhan River is dextrally displaced by around 12.6 km along the Büyükçay Fault Zone (Figure 11).

The southern and eastern margins display a step-like morphology. Along the southern margin, the vertical displacement is about 10 to 28 m, measured from the elevated and already fully formed travertine occurrences, and about 114 m to 160 m measured from terrace conglomerates on the footwall of the Büyükçay Fault Zone, as along the eastern central faults (Figure 7). As clearly shown, the eastern and southern margins underwent two phases of uplift (Figures 7, 9 & 12).

Asymmetrical river terrace conglomerates, 0.5 to 2 metres thick, are dominantly located at the centre, and the southern and eastern margins of the MS basin. These conglomerates are exposed at 20–40 metres in the centre of the basin and at around 160 m along the margins and some are tilted by a few degrees. Along the margins, the asymmetrical river terrace deposits were observed at 582 m, where the stream elevation is 510 m. Also, at the eastern end of the Uzunyazı Faults, west of Değirmendere village, the stream terrace deposits are located at a height of 672 m where the stream bed elevation is 450 m indicating a vertical uplift of 114 m. However, the average vertical uplift in the Quaternary terraces is around 150 m both in the eastern and southern margins. Three coeval asymmetrical fluvial terraces south of the MS basin are dated at between 109±7.4 ka and 32.4±4.4 ka (Kıyak & Erturaç 2008).
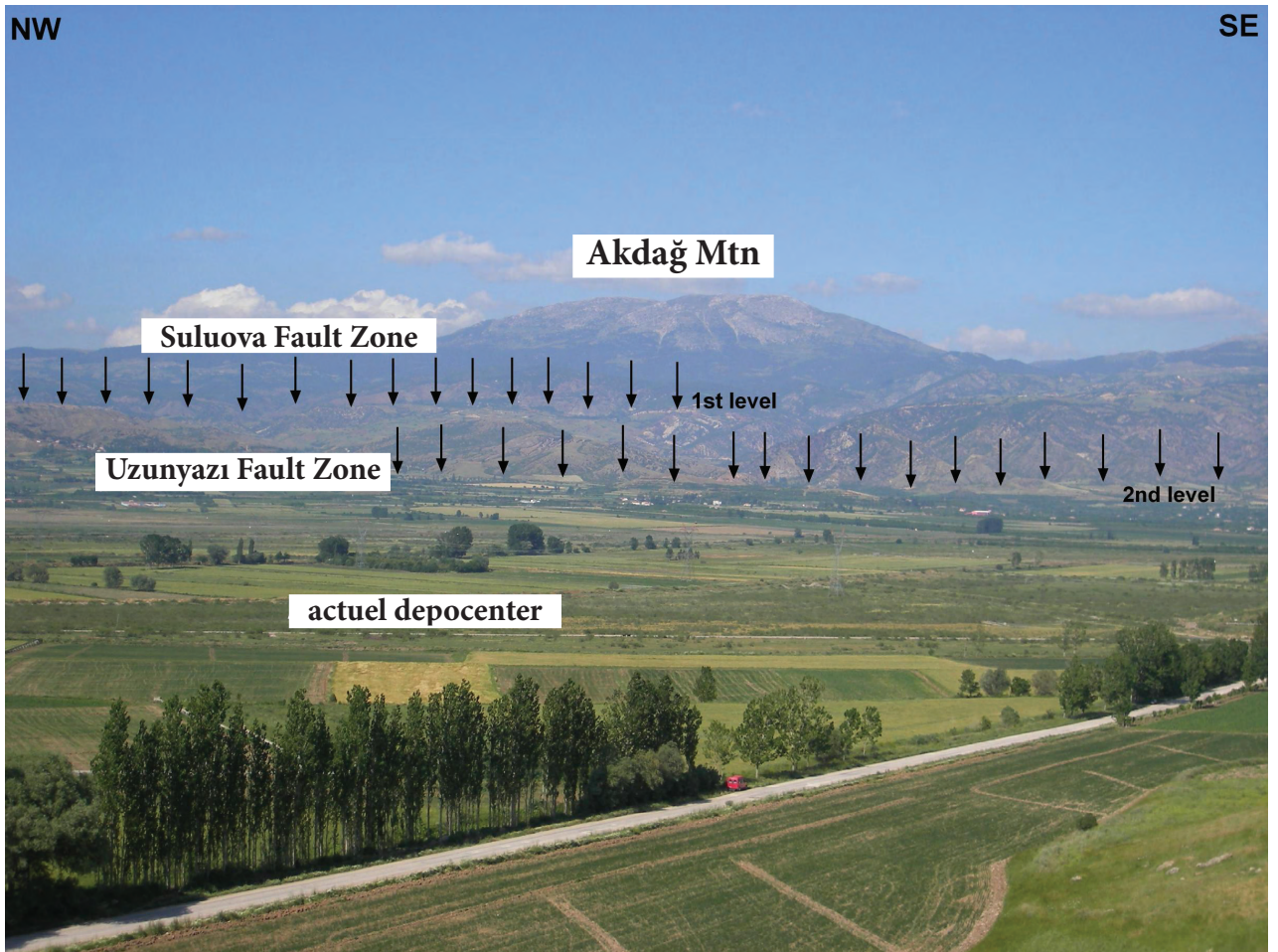
Figure 12. Paired terrace conglomerates developed along the control of the Suluova Fault Zone and the Uzunyazı Fault Zone. Location: Eastern margin of the MS Basin. S of Akdağ Mountain.

Different amounts of vertical uplift along the margins might shift the depocentre due to the tilt of the basin. The position of the actual depocentre indicates either a shift of the MS basin towards the southeast or that the basin tilted south-southeast (Figure 3). This resulted in the migration of the southward flowing Tersakan stream towards the east and its flow in a SE direction (Figure 3).

Basin Fill – The basin is filled by Plio–Quaternary fluvial to lacustrine sediments and Quaternary fluvial sediments (Figure 4). The Plio–Quaternary fill consists of marginal and basinal units. Marginal units are coarse-grained alluvial to fluvial clastics over 140 m thick, resulting from rapid sedimentation. The basinal units are fine-grained clastics with lacustrine

deposits, which are at least 50 m thick. However, the maximum thickness of the Plio–Quaternary fill is over 410 metres south of Merzifon (DSİ Report 1973). The 250–300 m upper part is represented by pebbly alluvial fan deposits stratigraphically overlying mudrocks where lateral lithological transitions exist between the sequences in various parts of the MS basin (DSİ Report 1973). The Quaternary fills are characterized dominantly by marginal units over 40 m thick, which are coarse-grained clastics of thick alluvial fans, aprons, active braided river plains, talus breccias, seasonal fluvial clastics and terrace conglomerates resulting from rapid and seasonal deposition. The Quaternary basinal units are fine-grained clastics of alluvial plains, marshes, meandering river clastics and seasonal playa lakes with a thickness of over 10 m. However, DSİ boreholes indicate that the total

thickness of the Quaternary basin fill is over 510 m (DSİ Report 1973).

The southward-flowing Tersakan stream is displaced in E–W direction in a meandering pattern in the southeastern part of the basin, the actual depocentre, and results in a widespread swamp development. At some other localities, elongated swampy areas also exist along linear fault-controlled depressions (Figure 3).

Some of the alluvial fans combined to form coalescent alluvial aprons. At the northern margin of the basin, alluvial fans are combine and overlap each other. These huge, alluvial fans, 250 to 300 m thick, are deeply dissected by creeks.

Analysis on Bedding Attitudes – A contour diagram (equal area lower hemisphere projection) prepared from 216 bedding planes of the Plio–Quaternary units indicates a broad fold axis striking at 85°N, an almost E–W trend. This statistically analyzed result indicates a possible 355°N aligned compressive principal stress direction, when supported with other results of kinematic analysis. The fold axes are seen to be parallel to the strikes of marginal faults (Figure 3). However, an older group of folds trending N10–20°E, oblique to the major faults, were observed along the margins of the MS basin. These folds are interpreted as bends associated with basement faulting. No folding was recorded in upper Quaternary sequences of the basin that are only tilted up to 10° in several faulted areas.

Pattern of Neotectonic Structures and Their Kinematic Interpretation – A weighted rose diagram of the neotectonic faults (lineament analysis) was prepared to understand the statistical distribution of the fault trends. Based on the length weighted rose diagram, a well-developed dextral strike-slip fault system is seen (Figure 13). It is clear that four major fault groups co-operated in the development of the MS basin. The first group of faults are parallel or subparallel to the NAFMS (1939, 1942, 1943 earthquake rupture lineaments) (Blumenthal *et al.* 1943; Blumenthal 1950). Others are the secondary synthetic (R), antithetic (R') faults and extensional (T) faults. The NW-trending ones are right-lateral synthetic and NE-trending ones are left-lateral antithetic faults. The splay faults (P-shear) are counted with master faults (Y-shear) which are parallel to the NAFMS. According to the Reidel shear terminology (Tchalenko & Ambraseys 1970), Y-shears trend N80°W and P-shears trend almost E–W (Merzifon, Çetmi, Uzunyazı, Eraslan, Büyükçay fault zones); poorly developed Reidel shear (R) trend N50°W, conjugate Reidel shear (R') (faults linking the Merzifon and Çetmi, Çetmi and Uzunyazı, Uzunyazı and Büyükçay fault zones) trend N20°E, and tension fracture faults (T) (Suluova Fault Zone) trend N25°W (Figure 13). The cumulative resulting principal stress axis is 335°N which is somehow diverted from previous principal stress orientations, such as 354°N obtained from earthquake epicentre fault plane solutions (Canıtez 1973), 330°N from statistically measured lineament analysis (Dirik 1994) and 330°N from fault plane solutions of faults developed in post-Miocene sequences (Rojay 1993). However, the principal stress orientation from the 1996 earthquake solution is approximately 338°N which agrees well with our results (Figure 14).

Fault Plane Slip Data Analysis – For analyses of the fault plane slip data, the software Angelier Direct Inversion Method (version 5.42) was used (Angelier 1979, 1984, 1991). About 221 slip lineation data were measured at 14 locations to differentiate the deformational phases and to calculate the directions of principal stresses in the area. 10 of those locations are situated on the major faults mapped in the basin (Figure 14). Others are located on the faults recorded in the Miocene (pre-Pliocene) sequences. The fault plane slip data analysis is based on the relationship between maximum stress orientation (σ_1) and minimum stress orientation (σ_3) which are the key interpretative elements. The σ_3 is reliable and clear when the phi values exceed 0.7 (close to 1), and σ_1 is clear when the phi values are less than 0.40 (close to 0). Additionally, when the R values are less than 0.50, the strike-slip fault is interpreted as transtensional and, when the R values exceed 0.50, interpreted as transpression. In the Angelier analysis, the data with question marks are excluded from the analysis.

Depending on the fault plane slip data analysis and field observations, the results show that: (i) a
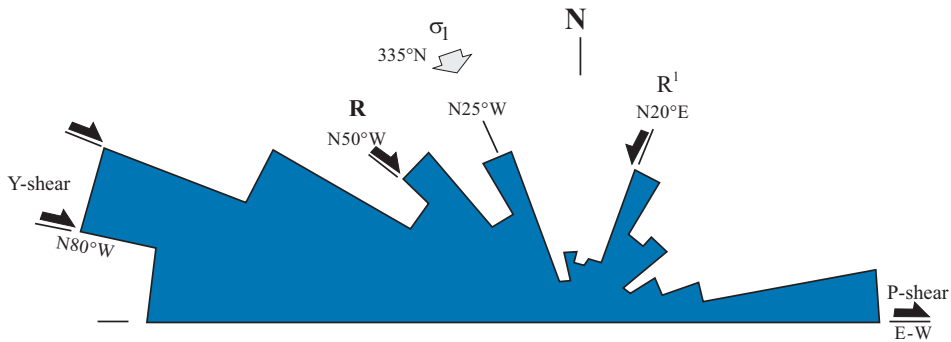
Figure 13. Weighted rose diagram showing dominant trends of the faults from lineament analysis based on 1:35,000 scale aerial photo analysis and field mapping, and major principal stress axis orientation (σ_1= 335°N) operating during the neotectonic evolution of the MS basin.

dextral strike-slip faulting with normal components is the latest motion, overprinted on to sinistral strike-slip faulting with reverse components along the Büyükçay Fault Zone (Figure 14, station 1) (Figure 11), (ii) dextral strike-slip faulting with reverse components along the western Uzunyazı Fault Zone (Figure 14, station 5), (iii) dextral strike-slip faulting with normal components along the Central and eastern Uzunyazı Fault Zone (Figure 14, station 2) (Figure 8), (iv) dextral strike-slip faulting with normal components along Merzifon Fault Zone (Figures 14 & 15, station 8), (v) normal faulting with dextral strike-slip component along the Suluova Fault Zone (Figure 14, station 9) and (vi) normal faulting with dextral strike-slip component as the initial motion which is overprinted by late dextral strike-slip faulting with normal components along the easternmost continuation of the Büyükçay Fault Zone (Figure 14, station 11).

The analysis done in the Miocene (pre-Plio–Quaternary) fill of the basin, found NW–SE to NE–SW compression, with manifestations of reverse faulting with minor strike-slip components (Figure 14; stations 3, 4; Figure 16). In contrast to pre-Plio–Quaternary faulting, almost E–W-trending normal faulting is recorded in Plio–Quaternary sequences (Figure 17). These are gentle faults active during Plio–Quaternary time, which did not affect the uppermost Quaternary units.

Overprinting relations of the slip lines on fault planes are rare. However, before running the data, it was clearly observed that dextral strike-slip faulting cut the normal, reverse and sinistral strike-slip faults in several locations (especially along the Büyükçay Fault Zone and along faults within the basin fills) during the collection of fault slip lineations. Therefore, the dextral strike-slip faulting postdated the normal, reverse and sinistral strike-slip faulting in the MS basin. The normal faulting is the oldest motion recorded in the Neogene configuration in the MS basin.

To sum up, the analysis indicated NE–SW and N–S extension (normal faulting) followed by NW–SE compression (reverse and left-lateral faulting). Lastly, under NW–SE compression, dextral faulting crosscut the entire region. The NE–SW extension might have occurred at the same time as the latest NW–SE-oriented compression, as the natural behaviour of the stress regime under NW–SE-oriented compression, causing a dextral movement. However, in the field studies, the crosscutting relationship clearly demonstrates that dextral faulting was the latest motion.

Seismicity – The MS basin is located within a seismically active region with significant activity during historical times (http://www.koeri.boun.edu.tr). The basin is bounded by seismically active faults: the master strand of the NAFZ to the north and by another important active strand to the south, the Ezinepazar splay of the NAFZ where the 1939 Erzincan earthquake occurred. The region between
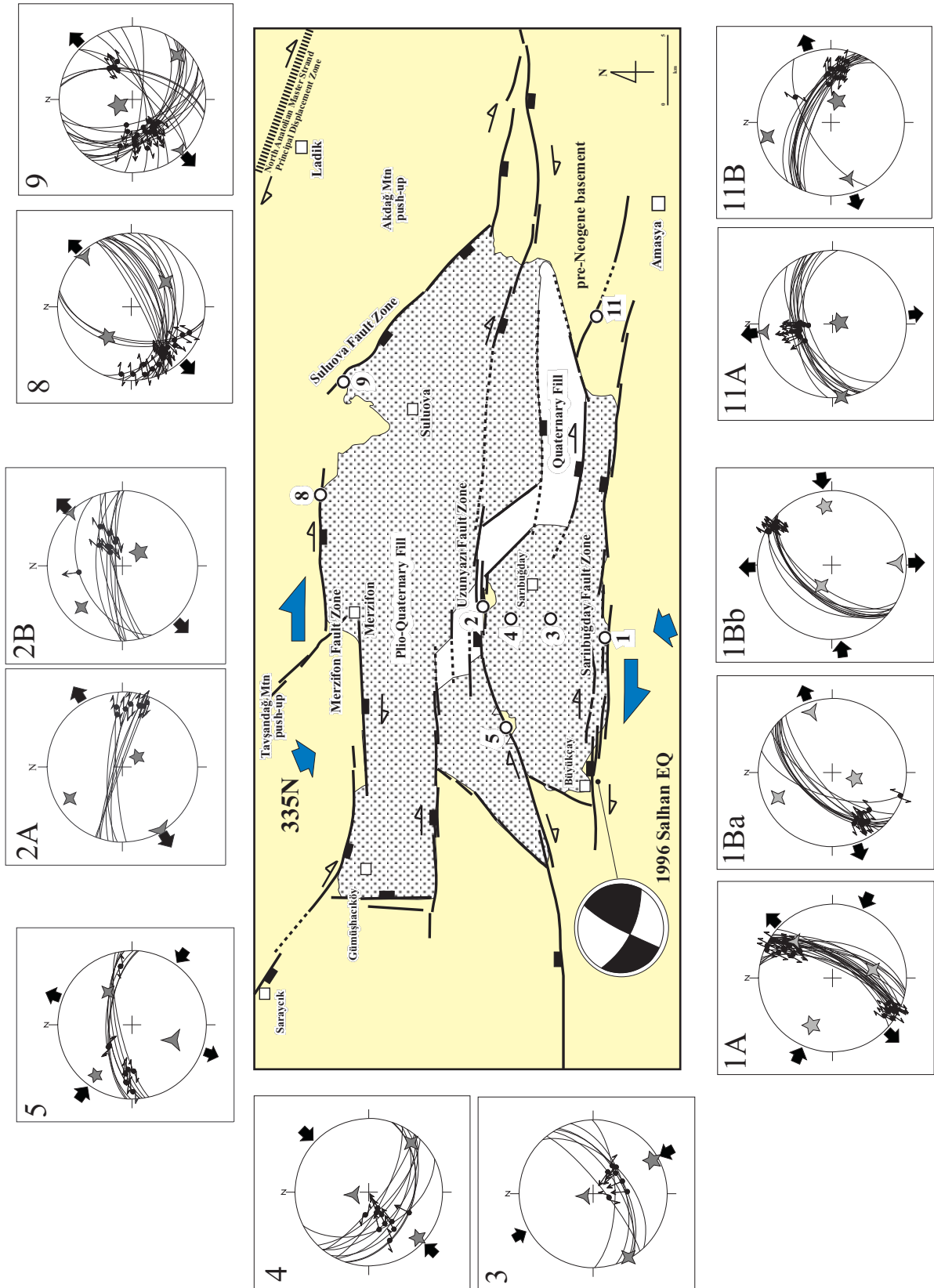
Figure 14. Simplified neotectonic map of the MS Basin with the stereo-plots of the principal stress directions obtained by analyses of the slip data for the post-Plio–Quaternary phase and the 1996 Salhan earthquake epicenter solution.

Figure 15. Slickenlines epicting dextral strike-slip faulting with a normal component along the Merzifon Fault Zone. Location: Kayadüzü village.

these fault zones is seismically active, as shown by recent earthquakes, especially the 1992 (15/02, M= 5.0) and 1996 (14/08, M= 5.2) earthquakes (Demirtaş 1996). The latest earthquake epicentre solutions manifest dextral strike-slip faulting along the southern margin with an approximately 338°N compression (Figure 14).

Discussion

Although there are contradictory views on the neotectonic evolution of the NAF system, especially on its initiation age, offset and rate of motion, we support a transtensional regime during the neotectonic period since the Pliocene in the MS basin. On an Eastern Mediterranean scale, the convergence between the Anatolian micro plate and the Afro-Arabian plate is accommodated by the displacement along the North and East Anatolian faults, resulting in the extension and anticlockwise rotation of the Anatolian micro plate between these

Figure 16. A thrust fault and unconformably overlying Plio–Quaternary sediments, suggesting pre-Plio–Quaternary compression. Location: E of Kamışlı village, along road cut.

Figure 17. Almost E–W-striking normal faulting along faults developed in Plio–Quaternary clastics. Location: Kamışlı village.

two intracontinental transform faults (Rotstein 1984; Hempton 1987; Gürsoy *et al.* 1999; Kaymakcı *et al.* 2003), as deduced from the indentation tectonics of the Himalaya system (Asian-Indian collision; escape of 'China block') (e.g., Molnar & Tapponier 1975; Tapponier 1977). The time of activation of the NAFZ as a single shear, which is coeval with the time of the last phase of 'rifting' (initiation of sea floor spreading; 5 to 4.5 Ma) in the Red Sea (Hempton 1987), was eased by the drift of Anatolian micro plate sliding along the East Anatolian and North Anatolian faults on to the African plate along the Mid-Mediterranean 'Ridge' during the Pliocene (5 Ma). Therefore, the Pliocene should be the time of activation of the

NAFZ as a single shear, which is the beginning of the neotectonic period in Anatolia.

This plate kinematics gave rise to the development of several neotectonic basins between and along the fault zones. However, the basins that are situated between these two intracontinental transform fault zones and their splays have much larger spatial distribution and superposed nature, as with the MS basin, when compared with those situated along the principal displacement zone of the fault zones.

The MS basin, located south of the master fault of the NAFZ and north of the Ezinepazarı splay fault of the NAFZ, has been segmented into several small pull-apart basins (sub-basins) and overprinted on to a pre-existing Miocene extensional basin, experienced a short-lived compression up to the end of the Miocene. Initially, several sub-basins appeared as a result of the initiation of faulting at the centre of the MS basin (Uzunyazı Fault Zone) during the Quaternary. As the slip on the faults increased, each small pull-apart basin randomly began to combine into a larger composite one during the latest Quaternary. The random coalescence and interaction processes in present sub-basins and regional uplifts/horsts (as a result of the bending of the NAFMS along possible palaeofaults; the northern domain Tavşandağ and Akdağ mountains, and the southern domain Amasya 'highland') resulted in a complex arrangement of sub-basins and tectonic domains, and the formation of a composite pull-apart basin (as proposed by Aydın & Nur 1982; Hempton 1982; Mann *et al.* 1983).

The MS basin is a large composite strike-slip basin. Although the ideal pull-apart basins are modelled to have a 1:3 ratio (Aydın & Nur 1982), the MS basin (2:5) and combined composite pull-apart basins (7:16) do not fit this ratio. The long duration of geological time and whether the basins are located along the principal displacement zone or not are important factors in having 1:3 ratios. The MS basin is outside the principal strike-slip displacement zone and has been active since the Miocene.

Regarding the development of the basin, the unconformity between the Miocene mudrocks and Plio–Quaternary clastics shows the existence of two basin infills. Field observations show the deformational difference in the intensity and style

of deformation between the Miocene and Plio–Quaternary sequences. The Miocene units are intensely folded and faulted, whereas the Plio–Quaternary clastics are gently folded, and where folded, broad open folding is characteristic. These observations support the superimposed nature of the MS basin.

Regarding the attitude of the active faults acting in the MS basin, the curvilinear trends, stepping and linking of faults are important products of the strike-slip faulting in the MS basin. The Suluova normal fault zone (Figure 14, no. 9) is a linkage zone between the northern margin, Merzifon (Figure 14, no. 8), and central, Uzunyazı-Taşova (Figure 14, no. 2) dextral strike-slip fault zones, indicating a NW–SE compression and NE–SW extension (Figure 14). The other fault zone typical of strike-slip faulting is the curvilinear central fault zone, the Uzunyazı Fault Zone. The ENE–WSW-trending western part of the zone displays a restoring bend (Figure 14, no. 5) and the WNW–ESE-trending eastern part displays a releasing bend (Rojay 1993). The stepping nature of the fault zone – especially along the southern margin Büyükçay fault zone (Figure 9) and eastern margin Suluova fault zone (Figure 12) are very clear. These might be the result of the release of stress at certain times during the Quaternary.

As well documented, dextral motion under NW–SE compression is the latest motion overprinted on normal and reverse faulting. The dextral displacements along the NAFZ have been discussed since Pavoni (1961). Displacements of 350–400 km (Pavoni 1961), 60–80 km since the Pliocene (Tokay 1973), 85±5 km since the Burdigallian (Seymen 1975), 100–120 km (Bergougnan 1975) and 25±5 km (Yılmaz 1985) have been proposed by measuring displaced geological units or the northern suture belt. However, the attitude of the displaced geological units and faults has not been counted in the calculations of the offsets, and this is an important omission. The 10 km displacement since the Pliocene has been proposed for many years against the offsets mentioned above (Ketin 1969). The latest displacement values along the master strand of the fault zone are: 25±5 km from displaced upper Miocene sequences in the Havza-Ladik area (Barka & Hancock 1984); 27 km

displacement on the NAFMS along the course of Kızılırmak River in Kamil town (Barka 1984), 7 km displacement in Vezirköprü town (Dirik 1994) and 15 km along the Çobanlı River in Suşehri town (Koçyiğit 1990). The displacement of the Salhan stream from an area located between the master strand of the NAFZ and the splay is measured at 12.6 km where the activity of the stream is presumed to be Pliocene (Figure 11). The displacement indicates a rate of 0.25 cm/year since the Pliocene (5 Ma), which is much less than the proposed slip rates obtained from the principal displacement zone of the NAFZ (e.g., Canıtez 1973; Barka & Gülen 1988; Koçyiğit 1989; Barka 1992). However, the displacement might have occurred between the Pliocene and Late Quaternary, calculated at a rate of between 0.25 to 0.63 cm/yr in the Merzifon-Suluova-Amasya region.

Also relevant to lateral displacement is the possible existence of relative reversal offsets, sinistral lateral displacements, since the Pliocene (Barka & Hancock 1984). These might be result of the local fault bounded block rotations where the faults control the MS basin evolution. This kind of reversal offset can exist along the western part of the Uzunyazı fault zone, explicable by re-positioning the Plio–Quaternary fill of the MS basin (Figures 3 & 14). However no fault-slip data recorded during the field surveys provide supporting evidence for such reversal displacements.

Vertical uplift is another important issue in the evolution of the MS basin. The existence of two asymmetrical fluvial terrace conglomerates at altitudes of 20–40 m within the basin and at as much as 160-m-along margins with leveled flat surfaces indicates two phases of vertical uplift during the Latest Quaternary. However, the lack of enough data on eustatic sea level changes in the Black Sea cause us to correlate the uplift amounts of the fluvial terraces with sea level changes.

The 109±7.4 ka to 32.4±4.4 ka age of the fluvial terraces (Kıyak & Erturaç 2008) indicates that latest Quaternary fault is active in the region. Another issue is the displacement of the Tersakan stream, which is younger than the youngest fluvial terraces, indicating that fault activity and the tilt of the MS basin is coeval with or younger than 32.4±4.4 ka.

Conclusions

A few final points include:

1. The unconformity between the Miocene and Plio–Quaternary and the intense deformation of the older, Miocene, infill compared to the Plio–Quaternary fill reveal the superimposed nature of the MS basin.

2. The statistical analysis of 216 bedding planes from the Plio–Quaternary units indicates a 355°N principal stress direction; from lineament analysis it is about 335°N; from fault plane solutions of faults developed in post-Miocene sequences it is about 330°N and is approximately 338°N from the epicentre solution analysis of the latest earthquake to take place in the region (Salhançayı earthquake 14/08/1996, M= 5.2). As proved from various structural analyses, the operating principal stress since the Pliocene agrees well.

3. The fault plane analysis done on 221 slip lineation data from the Miocene–Pliocene units using the Angelier Direct Inversion Method and field observations shows: (i) dextral strike-slip faulting with normal components as the latest motion overprinted onto sinistral strike-slip faulting with reverse components along the southern margin fault zone (Sarıbuğday Fault Zone), (ii) dextral strike-slip faulting with reverse components along the central fault zone (Uzunyazı Fault Zone), (iii) dextral strike-slip faulting with normal components along northern margin fault zone (Merzifon Fault Zone), and (iv) normal faulting with dextral strike-slip component along the eastern margin fault zone (Suluova Fault Zone). NW–SE compression is found as the latest principal stress orientation in the MS basin. The principal compressive stress orientation on the neotectonic NAFZ and MS basin is conformable, and latest earthquakes show that the stress regime acting in the region on the NAF system and the MS basin are the same.

4. The neotectonic dextral strike-slip deformation post-dates the normal faulting, reverse faulting, sinistral strike-slip faulting, post-Late Miocene folding and thrusting in the research area. Therefore, initiation of the dextral strike-slip deformation (Neotectonic deformation) should be post-latest Miocene, e.g. Pliocene on the North Anatolian Fault System.

5. The Salhan stream is dextrally displaced by 12.6 km by the Büyükçay Fault Zone along which the latest (1996) earthquakes took place. Along this fault zone, the vertical displacement is about 160 m. The rate of slip is proposed at 0.25 cm/yr since the Pliocene.

6. Regional vertical uplift produced the south-southeast tilt of the MS basin and resulted in the shift of the depocenter towards the southeast.

7. The early formed, Miocene rhomboidal basin is bisected by E–W-trending Plio–Quaternary faults. Coalescence of several parallel sub-basins along the E–W-trending Plio–Quaternary faults resulted in a composite pull-apart basin during the latest Quaternary.

Collectively, post-Miocene compression was followed by a post-Pliocene regionally continuous progressive transtension. The Pliocene is the time of initiation of strike-slip deformation in the region. The composite MS pull-apart basin evolved as a superimposed basin in a composite array in a post-Pliocene strike slip regime in which the basin developed on the pre-existing Miocene basin.

Acknowledgement

References

Aktİmur, H.T., Tekİrlİ, M.E. & Yurdakul, M.E. 1990. *Tokat-D2 Paftası, Türkiye Jeoloji Haritaları Serisi [Tokat D2 Sheet, Geological Map Series of Turkey]*. Mineral Research and Exploration Institute of Turkey (MTA) Publication.

Allen, C.R. 1982. Comparisons between the North Anatolian Fault of Turkey and the San Andreas Fault of California. *In*: Işıkara, A.M. & Vogel, A. (eds), *Multidisciplinary Approach to Earthquake Prediction*. Wiesbaden, Friedrich, Vieweg and Sohn, 67–85.

Angelier, J. 1979. Determination of the mean principal directions of stresses for a given fault population. *Tectonophysics* **56**, T17-T26.

Angelier, J. 1984. Tectonic analysis of fault slip data sets. *Journal of Geophysical Research,* **80**, 5835–5848.

Angelier, J. 1991. Inversion of field data in fault tectonics to obtain regional stress. III: a new rapid direct inversion method by analytical means. *Geophysical Journal International* **103**, 63–76.

Alp, D. 1972. *The Geology of Amasya and Surroundings*. PhD Thesis, İstanbul University, Faculty of Science Monographs **22** [in Turkish].

Arpat, E. & Saroğlu, F. 1975. Türkiye'deki bazı önemli genç tektonik olaylar [Some recent tectonic events in Turkey]. *Türkiye Jeoloji Kurumu Bülteni* **8**, 91–100.

Aydın, A. & Nur, A. 1982. Evolution of pull-apart basins and their scale independence. *Tectonics* **1**, 91–105.

Barka, A.A. 1984. Kuzey Anadolu Fay Zonu'ndaki bazı Neojen-Kuvaterner havzalarının jeolojisi ve tektonik evrimi [Geology and tectonic evolution of Neogene–Quaternary basins along the North Anatolian Fault Zone]. *In*: *Ketin Simpozyumu*, 209–227.

Barka, A.A. 1992. The North Anatolian Fault Zone. *Annales Tectonicae* **6**, 164–195.

Barka, A.A. & Gülen, L. 1988. New constraints on the age and total offset of the North Anatolian fault Zone: Implications for tectonics of the eastern Mediterranean region. *METU Journal of Pure and Applied Science Bulletin* **21**, 39–63.

Barka, A.A. & Hancock, P.L. 1984. Neotectonic deformation patterns in the convex-northward arc of the North Anatolian fault zone. *In*: Dixon, J.E. & Robertson, A.H.F. (eds), *The Geological Evolution of the Eastern Mediterranean*. Geological Society, London, Special Publications **17**, 763–774.

Bergougnan, H. 1975. Relations entre les edifices Pontique et Tourique dans le nord-est de l'Anatolie. *Bulletin of Geological Society of France* **7**, 1045–1057.

Blumenthal, M. 1945. Ladik deprem hattı [Ladik earthquake zone]. *Mineral Research and Exploration Institute of Turkey (MTA) Bulletin* **33**, 153–174.

Blumenthal, M.M. 1950. *Orta ve Aşağı Yeşilırmak Bölgelerinin (Tokat, Amasya, Havza, Erbaa, Niksar) Jeolojisi Hakkında [About the Geology of Central and Lower Yeşilırmak Regions (Tokat, Amasya, Havza, Erbaa, Niksar)]*. Mineral Research and Exploration Institute of Turkey (MTA) Geological Map Series **D/4**.

Blumenthal, M.M., Pamir, H.N. & Akyol, İ.H. 1943. Zur Geologie der Landstrecken der Erdbeben von ende 1942 in Nord-Anatolien und dortselbst ausgeführte makroseismische Beopachtungen [Şimal Anadolu zelzele sahasının jeolojisi ve 1942 yılı sonunda buralarda yapılan makro-sismik müşahedeleler]. *Mineral Research and Exploration Institute of Turkey (MTA) Bulletin* **29**, 33–58.

Bozkurt, E. & Koçyiğit, A. 1996. The Kozova basin: an active negative flower structure of the Almus Fault Zone, a splay fault system of the North Anatolian Fault Zone, Turkey. *Tectonophysics* **265**, 239–254.

Canitez, N. 1973. Yeni kabuk hareketlerine ilişkin çalışmalar ve Kuzey Anadolu Fay problemi [Research on recent crustal movements and North Anatolian Fault problem]. *Kuzey Anadolu Fayı ve Deprem Kuşağı Simpozyumu.* Mineral Research and Exploration Institute of Turkey (MTA) Special Bulletin, 35–38.

Demi̇rtaş, R. 1996. 14 Ağustos 1996 Salhançayı (Çorum-Amasya) depremi [14 August 1996 Salhançayı (Çorum-Amasya) earthquake]. *TMMOB Jeoloji Mühendisleri Odası Haber Bülteni* **96**, 13–16.

Di̇ri̇k, K. 1994. Kuzey Anadolu Transform Fay Zonu'nun Beşpınar-Havza kesimindeki neotektonik özellikleri [Neotectonic characteristics of North Anatolian Transform Fault Zone in Beşpınar-Havza section]. *Mineral Research and Exploration Institute of Turkey (MTA) Bulletin* **116**, 37–50 [in Turkish].

Dsi̇ report, 1973. *Merzifon-Gümüşhacıköy Ovası Hydrogeological Research Report.* Ankara [in Turkish, unpublished].

Genç, Ş., Kurt, Z., Küçükmen, O., Cevher, F., Saraç, G., acar, Ş., Bi̇lgi̇, C., Şenay, M. & Poyraz, N. 1993. *Merzifon (Amasya) Dolayının Jeolojisi [Geology of Merzifon (Amasya) Region].* Mineral Research and Exploration Institute of Turkey (MTA) Report no. **9527** [in Turkish, unpublished].

Gürsoy, H., Piper, J.D.A., Tatar, O. & Temi̇z, H.A. 1997. Paleomagnetic study of the Sivas Basin, central Turkey: crustal deformation during lateral extrusion of the Anatolian Block. *Tectonophysics* **271**, 89–105.

Harding, T.P. & Lowell, J.D. 1979. Structural styles, their plate tectonic habitats, and hydrocarbon traps in petroleum provinces. *Bulletin of American Association of Petroleum Geologists* **63**, 1016–1058.

Hempton, M.R. 1982. The North Anatolian Fault and complexities of continental escape. *Journal of Structural Geology* **4**, 502–504.

Hempton, M.R. 1987. Constraints on Arabian Plate motion and extensional history of the Red Sea. *Tectonophysics* **6**, 687–705.

Irrlitz, W. 1971. Neogene and older Pleistocene intramontane basins in the Pontic region of Anatolia. *Newsletter Stratigraphy* **3**, 33–36.

Kaymakci, N., White, S.H. & Van Dijk, P.M. 2003. Kinematic and structural development of the Çankırı Basin (Central Anatolia, Turkey): a paleostress inversion study. *Tectorophysics* **364**, 85–113.

Keti̇n, İ. 1969. Über die Nordanatolische Horizontalverschiebung. *Mineral Research and Exploration Institute of Turkey* **72**, 1–28.

Kiyak, N.G. & Erturaç, M.K. 2008. Luminescence ages of feldspar contaminated quartz from fluvial terrace sediments. *Geochronometria* **30**, 55–60.

Koçyiği̇t, A. 1989. Basic geological characteristics and total offset of North Anatolian Fault Zone in Suşehri area, NE Turkey. *M.E.T.U. Journal of Pure and Applied Sciences* **22**, 43–68.

Koçyiği̇t, A. 1990. Tectonic setting of the Gölova basin; total offset of the North Anatolian fault Zone, E Pontide, Turkey. *Annales Tectonicae* **IV**, 155–170.

Koçyiği̇t, A. 1996. Superimposed basins and their relations to the recent strike-slip fault zone: a case study of the Refahiye superimposed basin adjacent to the North Anatolian Transform Fault, northeastern Turkey. *International Geology Review* **38**, 701–13.

Koçyiği̇t, A. & Rojay, B. 1988. *Merzifon (Amasya) ve Geyve (Adapazarı) Bölgelerinde Kuzey Anadolu Fay Kuşağı'nın Revizyonu [Study of North Anatolian Fault Zone in Merzifon (Amasya) and Geyve (Adapazarı) Area].* M.E.T.U. Research Foundation Report no. 86-03-09-02 [in Turkish, unpublished].

Mann, P., Hempton, M.R., Bradley, D.C. & Burke, K. 1983. Development of pull-apart basins. *Journal of Geology* **91**, 529–554.

Molnar, P. & Tapponier, P. 1975. Cenozoic tectonics of Asia: effects of a continental collision. *Science* **189**, 419–426.

Öztürk, A. 1980. Ladik-Destek yöresinin tektoniği [Tectonics of Ladik-Destek region]. *Türkiye Jeoloji Kurumu Bulletin* **23**, 31–38 [in Turkish with English abstract].

Pavoni, N. 1961. Die Nordanatolische Horizontal-verschiebung. *Geologische Rundchau* **51**, 122–139.

Rojay, B. 1993. *Tectonostratigraphy and Neotectonic Characteristics of the Southern Margin of Merzifon-Suluova Basin, Central Pontides, Amasya.* PhD Thesis, Middle East Technical University [unpublished].

Rojay, B. 1995. Post-Triassic evolution of Central Pontides: Evidence from Amasya region, Northern Anatolia. *Geologica Romana* **31**, 329–350.

Rojay, B. & Koçyiği̇t, A. 2003. Outline, morphotectonic characteristics, total displacement and seismicity of the central North Anatolian fault System, Turkey. *International Workshop on the North Anatolian, East Anatolian and Dead Sea Fault Systems, Abstracts.* p. 85.

Rotstein, Y. 1984. Counterclockwise rotation of the Anatolian Block. *Tectonophysics* **108**, 71–91.

Seymen, I. 1975. *Kelkit Vadisi Kesiminde Kuzey Anadolu Fay Zonu'nun Tektonik Özelliği [Tectonic Characteristics of the North Anatolian Fault Zone in Kelkit Valley].* PhD Thesis, İstanbul Technical University, Faculty of Mines [in Turkish with English abstract, unpublished].

Şengör, A.M.C. 1980. *Türkiye'nin Neotektoniğinin Esasları [Fundemantels of Neotectonics of Turkey].* Türkiye Jeoloji Kurumu Conference Series **2**.

Şengör, A.M.C, Görür, N. & Şaroğlu, F. 1985. Strike slip faulting and related basin formation in zones of tectonic escape: Turkey as a case study. *In*: Christie-Blick, N. & Biddle, K. (eds), *Strike-slip Deformation, Basin Formation, and Sedimentation.* Society of Economic Paleontologists and Mineralogists, Special Publications **37**, 227–64.

Şengör, A.M.C., Tüysüz, O., İmren, C., Sakınç, M., Eyidoğan, H., Görür, N., Le Pichon X. & Rangin, C. 2005. The North Anatolian Fault: a new look. *Annual Review Earth Planetary Sciences* **33**, 1–75.

Şengör, A.M.C. & Yilmaz Y. 1981. Tethyan evolution of Turkey: a plate tectonic approach. *Tectonophysics* **75**, 181–243.

Sickenberg, O. & Tobien, H. 1971. New and lower Quaternary vertebrate faunas in Turkey, *Newsletter Stratigraphy* **3**, 51–61.

Sickenberg, O., Becker-Platen, J . D., Benda, L., Berg, D., Engesser, B., Gaziry, W., Heissig, K., Hunermann, K. A., Sondaar, P. **Y.,** Schmidt-Kittler, N., Staesche, K., Staesche, U., Steffens, P. & Tobien, H. 1975. Die Gliederung des höheren Jungtertiars und Altquatars in der Türkei nach Vertebraten und ihre Bedeutung für die internationale Neogen-Stratigraphie (Kanozoikum und Braunkohlen der Türkie 17). *Geologisches Jahrbuch* **B15**, 1–167.

Tapponier, D. 1977. Evolution tectonique du systeme Alpin en Mediterranee: Poinconnement et ecrasement rigide-plastique. *Bulletin of Geological Society of France* **3**, 437–460.

Tchalenko, J.S. & Ambraseys, N. 1970. Structural analysis of the Dasht-e Bayaz (Iran) earthquake fractures. *Geological Society of America Bulletin* **81**, 41–60.

Tokay, M. 1973. Kuzey Anadolu Fay Zonunun Gerede ile Ilgaz arasındaki kısmında jeolojik gözlemler [Geologic observations on the North Anatolian Fault Zone in then area between Gerede and Ilgaz]. *Kuzey Anadolu Fayı ve Deprem Kuşağı Simpozyumu*. Mineral Research and Exploration Institute of Turkey Special Publication, 12-29.

Tüysüz, O. 1996. Amasya ve çevresinin jeolojisi [Geology of Amasya and its surroundings]. *Türkiye 11. Petrol Kongresi, Proceedings*, Ankara, 32–48 [in Turkish with English abstract].

Yilmaz, A. 1985. Yukarı Kelkit çayı ile Munzur dağları arasının temel jeolojik özellikleri ve yapısal evrimi [Basic geological characteristics and tectonic evolution of the area between Upper Kelkit river and Munzur Mountains]. *Türkiye Jeoloji Kurumu Bülteni* **28**, 79–92 [in Turkish with English abstract).